

## PDF hosted at the Radboud Repository of the Radboud University Nijmegen

The following full text is a publisher's version.

For additional information about this publication click this link.

<http://hdl.handle.net/2066/175860>

Please be advised that this information was generated on 2019-05-20 and may be subject to change.

**Time-resolved nonlinear infrared spectroscopy of samarium ions in SmFeO<sub>3</sub>**D. Bossini,<sup>1,\*</sup> D. Malik,<sup>1</sup> B. Redlich,<sup>2</sup> A. F. G. van der Meer,<sup>1,2</sup> R. V. Pisarev,<sup>3</sup> Th. Rasing,<sup>1</sup> and A. V. Kimel<sup>1</sup><sup>1</sup>*Radboud University Nijmegen, Institute for Molecules and Materials, Heyendaalseweg 135, Nijmegen, The Netherlands*<sup>2</sup>*FOM-Institute Rijnhuizen, 3430 BE Nieuwegein, The Netherlands*<sup>3</sup>*Ioffe Physical-Technical Institute, Russian Academy of Sciences, 194021 St. Petersburg, Russia*

(Received 21 September 2012; revised manuscript received 11 January 2013; published 4 February 2013)

We demonstrate that resonant 32.3 THz pumping of  $f$ - $f$  transitions in the samarium ions in SmFeO<sub>3</sub> leads to a nonlinear regime of radiation-matter interaction. The nonlinearity arises from the photoinduced population of the excited state, the dynamics of which was studied in a pump-probe experiment. The measurements have been performed in the spectral range near the  ${}^6H_{5/2} \rightarrow {}^6H_{7/2}$  electronic transition. The observations show dynamics with a lifetime of 4 ps. The sign of the dynamics surprisingly differs in different spectral ranges: This phenomenon is interpreted as an excitation-induced shift of the spectral line. The results are described by the nonlinear optical polarization using the optical Bloch equations for an ensemble of two-level systems.

DOI: 10.1103/PhysRevB.87.085101

PACS number(s): 78.47.D—

Rare-earth orthoferrites form a wide class of well-known magnetic materials<sup>1–3</sup> that keep showing interesting and often unexpected phenomena in various areas of condensed matter physics.<sup>4,5</sup> For instance, recently orthoferrites have become a model system for the investigation of ultrafast photoinduced phase transitions,<sup>6,7</sup> a rather counterintuitive phenomenon in which a subtle perturbation, resonant with a specific mode of the solid, can result in dramatic changes of its electronic and magnetic state. Although most of the studies on this topic have been performed using near-infrared pumping,<sup>8,9</sup> the control with infrared radiation is an attractive opportunity, since this spectral range contains a large variety of collective modes. A selective pumping of one of these modes can trigger a phase transition consuming much less energy than in the case of a near-infrared stimulus. The understanding and realization of ultrafast and efficient photoinduced phase transitions in the orthoferrites is based on some crucial parameters, which have not been investigated yet. In fact, knowledge of the efficiency of pumping the transitions in the infrared domain, the lifetime of excitations, and nonlinearities appearing in light-matter interaction under intense, resonant laser excitation of an orthoferrite is still missing.

This paper constitutes a first step towards the addressing these issues. In particular, for this study we have chosen the orthoferrite SmFeO<sub>3</sub> and investigated the interaction of intense infrared radiation with the  ${}^6H_{5/2} \rightarrow {}^6H_{7/2}$  electronic transition in the Sm ion by means of the time-resolved infrared pump-probe technique.

The choice of this particular material and electronic transition was motivated by several reasons. First, orthoferrites are characterized by a rather unusual spin-reorientation phase transition (i.e., 90° rotation of the easy axis of magnetic anisotropy), which may be triggered by a temperature increase.<sup>10</sup> It is accepted that the phase transition occurs due to a temperature-induced repopulation of 4*f*-electronic states in the rare-earth ions.<sup>1</sup> Second, SmFeO<sub>3</sub> has the highest temperature of spin reorientation ( $T_{SR} = 456$  K) among all the orthoferrites.<sup>10</sup> Consequently, the electronic excitations responsible for the spin-reorientation phase transition have the highest energies and thus can be pumped at a shorter time scale. Third, we measured infrared absorption of SmFeO<sub>3</sub>

and from the spectrum that we report in Fig. 1, several lines can be seen in the range below 50 THz = 200 meV. We have chosen for our experiment the strongest one, centered at 32.3 THz = 133.3 meV, which has been identified as the  ${}^6H_{5/2} \rightarrow {}^6H_{7/2}$  transition.<sup>11</sup>

To resonantly excite SmFeO<sub>3</sub> with intense, ultrashort infrared laser pulses, we used the Free Electron Laser for Infrared Experiments (FELIX) in Nieuwegein (The Netherlands). In a pump-probe experiment we measured changes in transmittivity induced by infrared pumping as a function of time. Our sample was a 100 μm thick single crystal of SmFeO<sub>3</sub>, cut orthogonal to the [100] direction. The FEL delivered light pulses with a duration of about 4 ps and a bandwidth of about 0.45 meV (0.11 THz) that ensures the selective pumping of the  ${}^6H_{5/2} \rightarrow {}^6H_{7/2}$  transition, since the width of this line is estimated to be 1 meV (Fig. 1). The pump fluence was always set to 10 mJ/cm<sup>2</sup>. The light had linear polarization parallel to the [001] axis of the crystal along which the spins of Fe sublattices are oriented. The diameters of both the pump and probe beams focused on the sample were approximately 200 μm. Our experiment relied on a balanced-detection acquisition scheme. It involved a reference beam, with the same frequency and intensity as the probe pulse, undergoing the same optical path as the probe itself and delayed from it by 20 ns.<sup>12</sup> In order to study the dynamics of the aforementioned electronic Sm transition as a function of the excitation frequency, we varied simultaneously the energy of both the pump and the probe in a region centered around 133.3 meV. All our measurements were performed at 4 K. In Fig. 2(a) we plotted the normalized variation of the transmittivity  $\Delta T/T$ , at a time delay of 0.6 ps, where the spectral dependence of the signal is most pronounced.

In order to describe the physics underlying our data, we simulated the photoinduced changes in transmittivity by a model system. We note that the bandwidth of the FEL pulses is not narrow enough to resolve the fine structure of the excited state. Also, it is known that most of the  $f$ - $f$  electronic excitations, associated with the strongest spectral lines, correspond to the so-called *forced* electric dipole transitions.<sup>11</sup> Thus we performed the modeling by treating the sample as an ensemble of two-level systems coupled

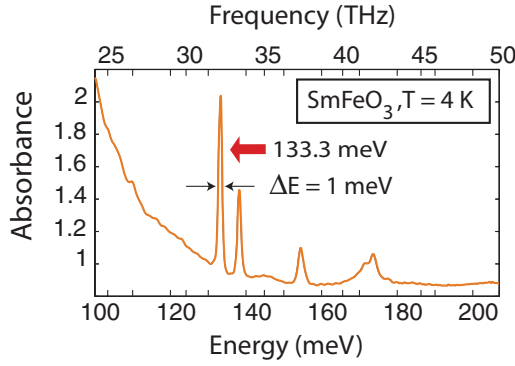


FIG. 1. (Color online) Absorption spectrum of  $\text{SmFeO}_3$  at 4 K measured with a Fourier transform infrared (FTIR) spectrometer. The range shown is between 100 meV ( $\sim 25$  THz) and 200 meV ( $\sim 50$  THz). The data are expressed in terms of absorbance, defined as the logarithm of the ratio between the intensity incident on the sample and the transmitted one. The red arrow indicates the  ${}^6H_5 \rightarrow {}^6H_7$  transition. We report also the full width at half maximum of the spectral line, indicated as  $\Delta E$  in the figure.

with light by electric dipole transitions. The possibility of a magnetic dipole transition cannot be ruled out *a priori*. However, our model did not take into account selection rules and thus similar simulations, performed for magnetic dipole transitions, would lead to similar results. We calculated the time-dependent transmittivity using the following equation:

$$\frac{\Delta T}{T} = \frac{\int dt |p_{\text{ref}}^{(1)}|^2 - \int dt |p_{\text{probe}}^{(1)} + p_{\text{pump}}^{(3)}|^2}{\int dt |p_{\text{ref}}^{(1)}|^2}, \quad (1)$$

where  $p_{\text{ref}}^{(1)}$  and  $p_{\text{probe}}^{(1)}$  are the first-order optical polarizations induced by the reference and probe beam, respectively, while  $p_{\text{pump}}^{(3)}$  is the nonlinear pump-induced polarization. The balanced-detection scheme implies that  $p_{\text{ref}}^{(1)} = p_{\text{probe}}^{(1)}$ .

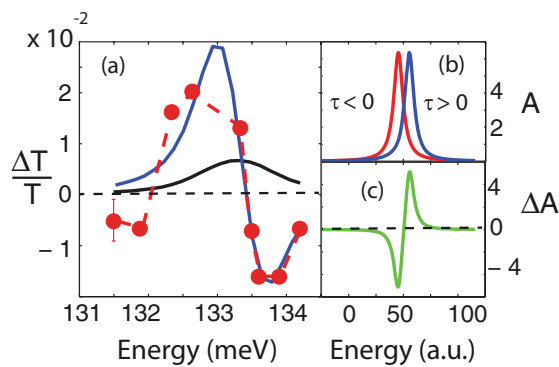


FIG. 2. (Color online) Photoinduced spectrum. (a) The red dots represent the experimental data and the red dashed line is a guide for the eye. The black curve shows the prediction of the weak-field model, while the blue line is the outcome of the extended model, which takes into account the self-energy correction. (b) The left ( $\tau < 0$ ) Lorentzian curve represents the unperturbed transition at 133.3 meV. The infrared pump pulse affects the transition frequency, thus the absorption line is blueshifted for positive delays (right curve). (c) Photoinduced modification of the absorption spectrum; the transmission spectrum can be obtained straightforwardly ( $1 - \Delta A$ ).

These polarizations were calculated using the optical Bloch equations,<sup>13</sup> since their intrinsic statistical nature makes them a suitable theoretical approach to model ensembles. The equations can be written as

$$\dot{n} + g_b n + (i/\hbar)(\Delta_{ba} p^* - p \Delta_{ba}^*) = 0, \quad (2)$$

$$\dot{p} + g p + (i/\hbar)\Delta_{ba}(1 - 2n) = 0, \quad (3)$$

where  $n$  and  $p$  are the diagonal and off-diagonal terms of the density matrix, therefore they represent the population of the excited state and the polarization of the material, respectively. The population of the ground state is  $1 - n$ . The two levels are indicated as  $a$  (ground state) and  $b$  (excited state),  $g_b$  is the inverse of the lifetime of  $b$  ( $T_1$ ),  $g = i(\Omega + d\Omega) + 1/T_2$  with  $\Omega = (E_b - E_a)/\hbar$ ,  $d\Omega$  is the detuning from the resonance frequency, and  $T_2$  is the dephasing time.  $\Delta_{ab}$  is the interaction energy between the electric field of light and the two-level system, in the electric dipole approximation.

To solve the coupled equations (2) and (3) we expanded the components of the density matrix into a Taylor series in the incident field amplitude, following Ref. 13. We assumed that in the absence of any perturbation the excited state is completely unpopulated and the medium has vanishing permanent optical polarization, which means  $n^{(0)} = p^{(0)} = 0$ . We chose the initial conditions  $n = 0$  and  $p = 0$ , which imply that the odd powers of  $n$  and the even powers of  $p$  are zero.<sup>13</sup> We calculated thus the polarization induced by the reference  $p_{\text{ref}}^{(1)}$  and the probe beam  $p_{\text{probe}}^{(1)}$  by means of the relation

$$\dot{p}^{(1)} + g p^{(1)} + (i/\hbar)\Delta_{ba} = 0. \quad (4)$$

The intensity of these two beams was so low that the interaction with the material could be described in terms of linear response. As a consequence no further terms in the expansion of the polarization are required. On the contrary, the electric field of the pump pulses drove the system into a nonlinear regime of interaction with light, which demanded to include the third-order term in the polarization that can be expressed as

$$\dot{p}_{\text{pump}}^{(3)} + g p_{\text{pump}}^{(3)} - 2(i/\hbar)\Delta_{ba} n^{(2)} = 0. \quad (5)$$

Here  $n^{(2)}$  is the second-order term in the expansion of the population, which is calculated from

$$\dot{n}^{(2)} + g_b n^{(2)} + (i/\hbar)(\Delta_{ba} p^{*(1)} - p^{(1)} \Delta_{ba}^*) = 0. \quad (6)$$

To test this theoretical scheme, which is known in the literature as *weak-field approximation*, we compared the  $\Delta T/T$  value, at a delay of 0.6 ps, from the calculated transmittivity dynamics [Eq. (1)] with the experimental data. As it can be seen in Fig. 2(a), the predictions of the weak-field model are inadequate.

Aiming to understand the origin of such a discrepancy, we modified our model [specifically Eq. (5)]. In principle, the  $f$  electrons are shielded from perturbations induced by the environment, because they are situated in an inner shell. However, the frequencies of these transitions depend on the surrounding electric fields. In particular, the excitation of a  $4f$  electronic transition in the Sm ion induces a modification in the *internal* electric field, which surrounds all the other Sm ions, as already reported.<sup>14</sup> The origin of this change in the electric

field has been ascribed<sup>15</sup> to the difference between the electric distributions of the ground and excited state. The modified electric field induces a Stark effect in the other Sm ions. As a consequence, the frequencies of the same  $f$ - $f$  transitions of these rare-earth ions become shifted. This scenario demands to take into account Sm-Sm many-body interactions. We chose for the self-energy an expression similar to the form introduced for the description of photoinduced processes in semiconductors.<sup>16</sup> In this extended version of the Bloch equations, Eq. (5) includes a correction term, representative for the energy shift of the transition,

$$g = i(\Omega + d\Omega + An^{(2)}) + \frac{1}{T_2}, \quad (7)$$

where  $A$  is the amplitude coefficient of the correction term. This equation accounts for the fact that the energy shift of the level is caused by the influence of the photoinduced population in the excited state on the system itself. The results of this model are plotted in Fig. 2(a) (blue line) and are in agreement with the experimental data. Thus we can interpret our results in terms of the excitation-induced frequency shift of the  $f$ - $f$  transition. To achieve a satisfactory description of the observations we tuned the value of some parameters, namely,  $A$ ,  $T_2$ , and  $\Delta_{ba}$ .

We note that if we model a medium as an ensemble of two-level systems, such nonlinear optical processes as the optical Stark effect and the dressed states picture cannot account for the observed spectral dependence of the transient transmittivity [Fig. 2(a)]. In our experiment only the blueshift of the spectral line has been observed, regardless of the excitation energy used. The aforementioned processes predict a blueshift of the line for pump energy lower than the resonant transition, and a redshift is expected in the case of excitation above the transition.<sup>17</sup>

We would like to underline that in Ref. 18 a similar blueshift was observed under intense infrared laser excitation, with photon energies below and above the resonance. The authors have described this shift in terms of dressed states, despite the fact that modeling of the effect, for an ensemble of two-level systems, gives a totally different spectral dependence of this shift.<sup>17</sup> It is important to mention that one cannot fully rule out alternative mechanisms of the blueshift, similar to those based on Autler-Townes splitting, since they are relevant for ensembles of three-level systems. However, a modeling of the effects in such ensembles is a more advanced problem, which is beyond the scope of this work. In this framework we decided to stay with a model based on a two-level system approach, including a self-energy correction which was not considered in Ref. 18.

Figures 2(b) and 2(c) show how in our model the infrared radiation affects the spectrum of the material: The first describes the photoinduced energy shift of the  $f$ - $f$  line, while the last gives the modification of the sample's transmittivity, which was the detected quantity in the experiment. Since  $A$  and  $n^{(2)}$  are both positive, the shift of the spectral line occurs always towards higher energies, in agreement with previous observations.<sup>18,19</sup>

In order to verify the validity of the model even further, the pump-induced transmittivity dynamics was calculated using Eq. (1) and it was plotted with the data in Fig. 3. A good

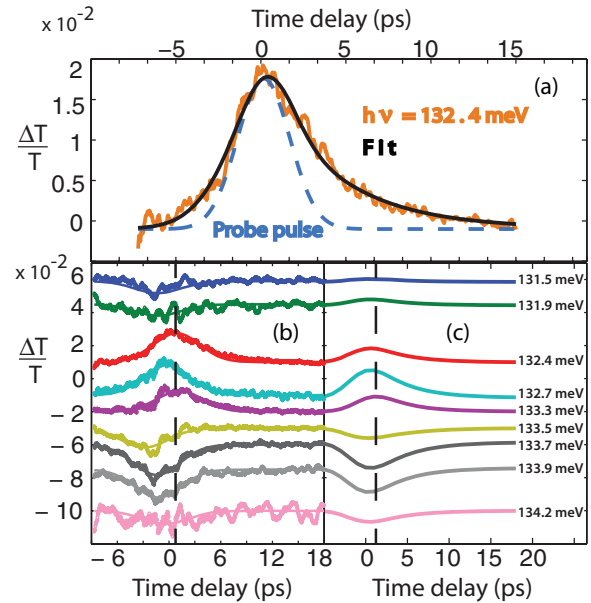


FIG. 3. (Color online) Time dependencies of the photoinduced transmittivity. (a) Experimental results obtained at a photon energy of 132.4 meV. The black line is a fit to the experimental data, revealing a 4 ps long decay time. The fit function used is reported in Ref. 21. The time profile of the probe pulse shows the experimental time resolution. (b) Measurements performed for different infrared radiation energies. The dashed black line shows the time delay at which the transmittivity has been extracted and compared with our model. The solid lines are guides for the eye. (c) Time-resolved transmittivity traces calculated using Eq. (1). The dashed black line shows the time delay at which the transmittivity has been extracted and compared with the data. The predictions of the model are in good agreement with the experimental observations.

agreement between the experimental evidence and the model is obtained by setting the maximum energy shift, which corresponds to the condition of resonant pumping, to  $1.2 \times 10^{-2}$  meV. This value is comparable with the calculations performed for Eu electronic transitions: In fact, since the Sm-Sm distance is  $\sim 5 \text{ \AA}$ ,<sup>20</sup> a frequency shift larger than 1 GHz can be expected.<sup>15</sup> The parameters  $\Delta_{ba}$  and  $A$  were adjusted to reproduce the observed 2% change in transmittivity. The values of  $T_1$  and  $T_2$  were  $T_1 = (4 \pm 0.4)$  ps and  $T_2 = (1 \pm 0.2)$  ps. The population decay time ( $T_1$ ) was obtained by fitting the time-domain data [Fig. 3(a)] with exponential functions. On the other hand, the dephasing time ( $T_2$ ) was a fit parameter of the model, the guess value (4 ps) of which was derived from the bandwidth of the absorption line shown in Fig. 1. The final and the guess values are comparable, which is a sign of consistency of the model. Moreover, the calculated  $\Delta T/T$  at 0.6 ps was compared with the data, as reported in Fig. 2(a). The change of transmittivity herein is consistent with the measurements: For energies lower than 133.3 meV, the transmittivity increases, while it decreases for higher energies. A similar effect for Dy, in dysprosium aluminum garnet, has been measured by optical absorption spectroscopy.<sup>19</sup>

From the data reported in Fig. 3(b) it appears that the transient change of transmittivity, which amounts to 2% of the static value, presents dynamics that relaxes in  $T_1 \sim 4$  ps. A comparison of this value with the time scale of the Sm-Fe

spin-spin interaction would determine whether the selective pumping of the 133.3 meV line could affect the magnetic state of the medium. In fact, once the  $4f$ -electronic states are repopulated, the spin reorientation is triggered in rare-earth orthoferrites by the spin-spin interaction between the rare-earth and the Fe ions.<sup>22</sup> In the case of  $\text{ErFeO}_3$  the value for the Er-Fe spin-spin interaction  $E_{\text{Er-Fe}}$  has been experimentally obtained.<sup>23</sup> From this parameter it is straightforward to derive the time scale of this interaction, which results in  $\tau_{\text{Er-Fe}} \sim \hbar/E_{\text{Er-Fe}} \sim 10$  ps. We may assume that the time scale of the interaction for Sm-Fe ( $\tau_{\text{Sm-Fe}}$ ) in our material is comparable to  $\tau_{\text{Er-Fe}}$ . We can thus state that the selective pumping of the  ${}^6H_{5/2} \rightarrow {}^6H_{7/2}$  transition induces dynamics on the same time scale as the Sm-Fe spin-spin interaction, which drives<sup>22</sup>

the spin-reorientation phase transition in rare-earth orthoferrites. Hence our experimental results are in favor of the idea of triggering the magnetic phase transition via the selective excitation of the  ${}^6H_{5/2} \rightarrow {}^6H_{7/2}$  Sm transition. To verify this scenario a pump-probe experiment should be performed, pumping the  ${}^6H_{5/2} \rightarrow {}^6H_{7/2}$  electronic transition and probing the magnetic response of the iron sublattices. This is possible by measuring the magneto-optical signal, for instance, Faraday rotation, in the visible and near-infrared spectral ranges.

This research was partially supported by de Nederlandse Organisatie voor Wetenschappelijk Onderzoek (NWO) and de Stichting voor Fundamenteel Onderzoek der Materie (FOM). R.V.P. thanks RFBR for support.

\*d.bossini@science.ru.nl

<sup>1</sup>R. L. White, *J. Appl. Phys.* **40**, 1061 (1969).

<sup>2</sup>A. V. Kimel, A. Kirilyuk, P. A. Usachev, R. V. Pisarev, A. M. Balbashov, and T. Rasing, *Nature (London)* **435**, 655 (2005).

<sup>3</sup>S. Artyukhin, M. Mostovoy, N. P. Jensen, D. Le, K. Prokes, V. G. de Paula, H. N. Bordallo, A. Maljuk, S. Landsgesell, H. Ryll, B. Klemke, S. Paegel, K. Kiefer, K. Lefmann, L. T. Kuhn, and D. N. Argyriou, *Nat. Mater.* **11**, 694 (2012).

<sup>4</sup>J. H. Lee, Y. K. Jeong, J. H. Park, M. A. Oak, H. M. Jang, J. Y. Son, and J. F. Scott, *Phys. Rev. Lett.* **107**, 117201 (2011).

<sup>5</sup>Y. Tokunaga, S. Iguchi, T. Arima, and Y. Tokura, *Phys. Rev. Lett.* **101**, 097205 (2008).

<sup>6</sup>A. V. Kimel, B. A. Ivanov, R. V. Pisarev, P. A. Usachev, A. Kirilyuk, and T. Rasing, *Nat. Phys.* **5**, 727 (2009).

<sup>7</sup>J. A. de Jong, I. Razdolski, A. M. Kalashnikova, R. V. Pisarev, A. M. Balbashov, A. Kirilyuk, T. Rasing, and A. V. Kimel, *Phys. Rev. Lett.* **108**, 157601 (2012).

<sup>8</sup>F. Cilento, C. Giannetti, G. Ferrini, S. Dal Conte, T. Sala, G. Coslovich, M. Rini, A. Cavalleri, and F. Parmigiani, *Appl. Phys. Lett.* **96**, 021102 (2010).

<sup>9</sup>G. Coslovich, C. Giannetti, F. Cilento, S. Dal Conte, G. Ferrini, P. Galinetto, M. Greven, H. Eisaki, M. Raichle, R. Liang, A. Damascelli, and F. Parmigiani, *Phys. Rev. B* **83**, 064519 (2011).

<sup>10</sup>N. Koshizuka and K. Hayashi, *J. Phys. Soc. Jpn.* **57**, 4418 (1988).

<sup>11</sup>G. Dieke, *Spectra and Energy Levels of Rare Earth Ions in Crystals* (Interscience, New York, 1968).

<sup>12</sup>P. C. Findlay, C. R. Pidgeon, R. Kotitschke, A. Hollingworth, B. N. Murdin, C. J. G. M. Langerak, A. F. G. van der Meer, C. M. Ciesla, J. Oswald, A. Homer, G. Springholz, and G. Bauer, *Phys. Rev. B* **58**, 12908 (1998).

<sup>13</sup>J. Shah, *Ultrafast Spectroscopy of Semiconductors and Semiconductor Nanostructures*, Springer Series in Solid-State Sciences, Vol. 115 (Springer, Berlin, 1999).

<sup>14</sup>S. B. Altner, G. Zumofen, U. P. Wild, and M. Mitsunaga, *Phys. Rev. B* **54**, 17493 (1996).

<sup>15</sup>N. Ohlsson, R. K. Mohan, and S. Kroll, *Opt. Commun.* **201**, 71 (2002).

<sup>16</sup>H. Haug and S. Koch, *Quantum Theory of the Optical and Electronic Properties of Semiconductors* (World Scientific, Singapore, 2009).

<sup>17</sup>Y. R. Shen, *The Principles of Nonlinear Optics* (Wiley, New York, 1984).

<sup>18</sup>A. Mysyrowicz, D. Hulin, A. Antonetti, A. Migus, W. T. Masselink, and H. Morkoç, *Phys. Rev. Lett.* **56**, 2748 (1986).

<sup>19</sup>A. H. Cooke, K. A. Gehring, M. J. M. Leask, D. Smith, and J. H. Thornley, *Phys. Rev. Lett.* **14**, 685 (1965).

<sup>20</sup>S. Geller and E. A. Wood, *Acta Crystallogr.* **9**, 563 (1956).

<sup>21</sup>A. V. Kimel, F. Bentivegna, V. N. Gridnev, V. V. Pavlov, R. V. Pisarev, and T. Rasing, *Phys. Rev. B* **63**, 235201 (2001).

<sup>22</sup>L. Chen, T. W. Li, S. X. Cao, S. J. Yuan, F. Hong, and J. C. Zhang, *J. Appl. Phys.* **111**, 103905 (2012).

<sup>23</sup>R. Faulhaber, S. Hüfner, E. Orlich, and H. Schuchert, *Z. Phys.* **204**, 101 (1967).